University of North Carolina Asheville
Journal of Undergraduate Research
Asheville, North Carolina
May 2021

Covalent Inhibition of Quorum Sensing in Biofilms

Jake Wilkinson
Chemistry & Biochemistry
The University of North Carolina Asheville
One University Heights
Asheville, North Carolina 28804 USA

Faculty Advisor: Dr. Caitlin McMahon

Abstract

One solution to the ever-growing problem of antibiotic resistance is antivirulence, a process which aims to disarm bacteria rather than kill them. A common virulence factor is the formation of biofilms, in which bacteria come together to form a community that protect themselves from antibiotics. Biofilms form through communication between bacteria by a process known as quorum sensing. During quorum sensing, bacteria synthesize and secrete signaling molecules known as autoinducers. Once a certain concentration threshold of autoinducers is reached, the bacteria begin to express genes that lead to biofilm formation. The synthesis of one quorum sensing molecule, autoinducer-2, is catalyzed by the enzyme LuxS, which is conserved throughout many species of bacteria. This reaction involves a cleavage of the natural substrate, S-ribosyl-L-homocysteine, into L-homocysteine and 4,5-dihydroxy-2,3-pentanedione. Inhibition of this reaction has previously succeeded through mimicking the natural substrate. To achieve more effective inhibition, and explore the possibility of a new strategy, a derivative of the natural substrate has been synthesized by combining L-homocysteine with an electrophilic group to promote formation of a covalent bond in the enzyme binding site and act as an irreversible inhibitor. A synthetic route to this derivative commenced by protecting the acid and amine of L-homocystine as a methyl ester and a carbamate, and by protecting the alcohols of D-erythronolactone with tert-butyldimethylsilyl chloride. This lactone was reduced, subjected to a Wittig reaction, and coupled to homocysteine and deprotected to introduce an α,β-unsaturated carbonyl as the electrophile for reaction with LuxS binding site cysteine. The *luxs* gene has been introduced to a pET-22b(+) plasmid to be expressed in E. coli cells so that the enzyme can be purified for enzyme activity assays.

1. Introduction

In the current age, antibiotic resistant infections have become an increasing problem. As stated by the Centers for Disease Control, at least 2.8 million people in the United States contract an infection each year in which bacteria are resistant to the antibiotics used against them.[1] Because effective treatment cannot be given to eradicate these infections, they are persistent and at least 35,000 people die each year in the United States as a result.[1] Antibiotics target specific bacteria in order to kill them, which places great selective pressure on that specific strain of bacteria to evolve with resistance to the administered antibiotic due to natural selection. Bacteria then quickly spread this resistance since they are capable of horizontal gene transfer, which refers to the ability of bacteria to trade genetic material with other bacteria without having to reproduce.[2] The rise of antibiotic resistance is increasing rapidly; resistance has been demonstrated as soon as one year after introduction of an antibiotic.[1] In light of this quick and dire progression, other strategies are needed in order to combat antibiotic resistance. Breakthroughs in studies of antivirulence point to it being a promising new strategy.

Antivirulence refers to the process of targeting virulence factors in order to disarm bacteria rather than kill them.[3] Virulence factors encompass a wide range of molecules that a bacterium can produce in order to increase effectiveness at infecting a host.[2] Examples of these factors include adhesins, regulators such as autoinducers, toxins, siderophores,

and other molecules that promote biofilm formation.[2] By targeting these virulence factors, there lies hope of being able to circumvent evolutionary selective pressure.[3] Unlike antibiotics, antivirulent treatments do not kill bacteria, but rather disarm them, decreasing pathogenicity and the likelihood for bacteria to evolve resistance to the antivirulent molecule. In addition, a benefit of antivirulent agents is the fact that they may be more selective toward pathogenic bacteria over commensal bacteria, another improvement over antibiotics.[3]

A virulence factor common to many bacteria is the formation of biofilms. Biofilms are best described as a lifestyle of bacteria in which multiple cells aggregate and are surrounded by a self-produced extracellular matrix.[4] The process of biofilm formation consists of attachment to a surface, followed by accumulation of bacteria to form a colony, and then colony maturation to a tower-like structure (Figure 1).[4,5] The formation of this mass community has many benefits to the bacteria.[4,5] Biofilms allow the bacteria survive conditions like starvation or dessication and serve as added protection against the host's immune system. In addition, biofilms contribute to a bacterium's resistance to antibiotics and can increase their resistance as much as 1,000-fold.[4] Biofilms increase antibiotic resistance of the community through a multitude of ways. For example, growth and metabolic acitvity is striated within a biofilm so that there is high activity near the outer layer but low activity near the center. Slow growth is beneficial against antibiotics, such as β-lactams, that only work when cells are actively growing. The extracellular matrix provides a physical barrier for antibiotics and often gene expression changes within a biofilm to upregulate efflux pumps that will excrete any antibiotics that does make it past the barrier. These factors allow biofilms to contribute to chronic infections and resistance.[5] For example, cystic fibrosis is a chronic multi-organ disease caused by genetics that leads to abnormal mucus in the lungs and persistant immune response. Dehydrated mucus within the airways of the lungs allows for bacteria to settle inside these airways, and cystic fibrosis patients often have chronic *Pseudomonas aeruginosa* infections. In these infections, *P. aeruginosa* is found almost exclusively as aggregates in a biofilm within the mucus of the lungs, which makes these infections difficult to treat.[6] Biofilms can also be found on medical equipment, such as catheters, stents, and even implants. Bacteria most commonly found on such devices are *Enterococcus faecalis*, *Staphylococcus aureus*, *Staphylococcus epidermidis*, *Steptococcus viridans*, *Escherichia coli*, and *P. aeruginosa*. These medical devices are made up of many different materials such as metals, polymers, ceramics, and composites depending on the type of device. These materials offer a surface for attachment of bacteria and subsequent biofilm formation. Biofilm growth on these devices within humans can cause infections that can often be life threating or cause the device to not work, causing more complications. Treatment for these infections requires high doses of antibiotics, which only perpetuates resistance development in these bacteria.[7]

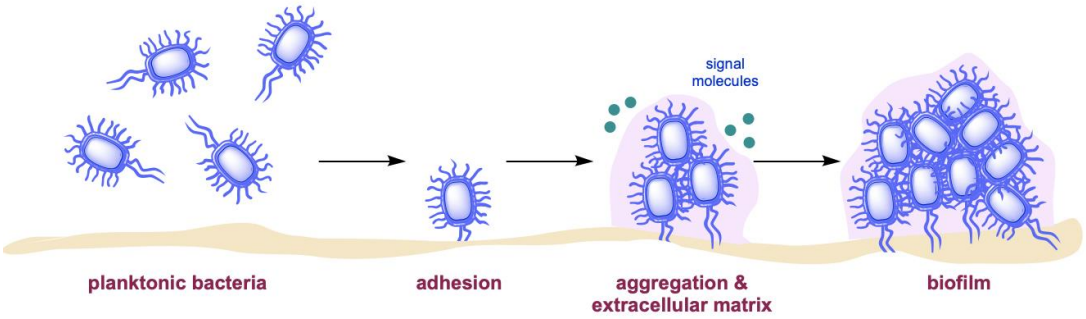

Figure 1. Steps of biofilm formation (McMahon).

Because biofilms are robust bacterial communities that occur in a wide range of diseases, the development of methods to inhibit the growth of biofilms is vital. Methods to inhibit biofilms include targeting adhesive organelles, carbohydrate binding adhesins, and quorum sensing.[8] Quorum sensing refers to cellular communication between bacteria, in which a concentration threshold of signaling molecules must be met in order to signal the bacteria to express genes that promote biofilm formation (Figure 2).[8,9] Quorum sensing mechanisms are found throughout both gram negative and gram positive bacteria.[9] Gram negative bacteria use a quorum sensing pathway in which acylated homoserine lactones (AHL) are produced as signaling molecules. AHLs then bind to the receptor LuxR, which can subsequently bind and remove a DNA repressor in order to allow expression of biofilm formation genes.[8] Another pathway of interest originally found in *Vibrio harveyi* bacteria is the synthesis of the signaling molecule autoinducer-2 (AI-2) catalyzed by the enzyme LuxS.[9] This reaction is important because the LuxS enzyme is found in both gram negative and gram positive bacteria and the signaling pathway allows for interspecies communication.[9] The AI-2

pathway has been reported in about half of all bacterial species, thus making it an ideal broad spectrum target of biofilm inhibition.[10]

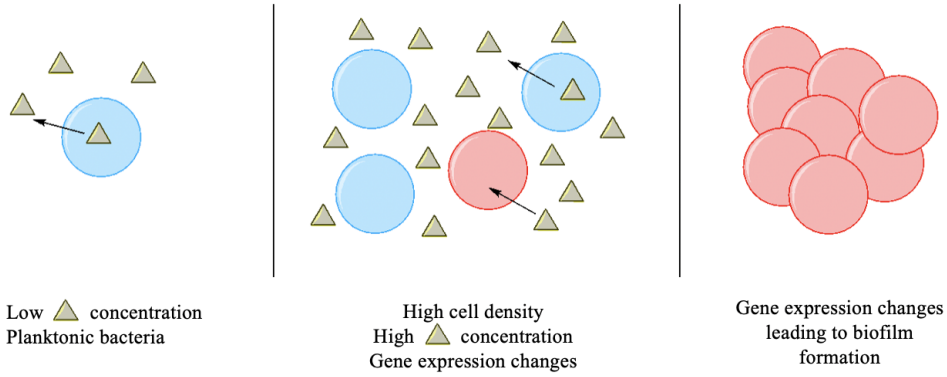

Figure 2. Schematic of quorum sensing mechanism. The triangles represent signaling molecules synthesized by bacteria. The change from blue to red represents the change in gene expression via signaling molecules (McMahon).

The AI-2 pathway was first described in *V. harveyi*, a marine bacterium.[11] The pathway involves LuxS catalyzing the cleavage of the natural substrate , S-ribosyl-L-homocysteine (SRH) into two different molecues, L-homocysteine and 4,5-dihydroxy-2,3-pentanedione (DPD) (Figure 3).[10] DPD is the crucial precursor to AI-2. DPD will undergo spontaneous cyclization, and will react with borate in the environment to form AI-2.[11] Though this pathway allows for interspecies communication, there are differences in the pathway between species. Borate is abundant in marine environments, however, other species utilize different derivatives of DPD as the signaling molecule, so not all signaling molecules contain boron.[11] In addition, LuxS contains a metal for coordination, which can either be Fe^{2+} or Zn^{2+} depending on the species.[12,13] However, two important amino acids found within the binding site are found highly conserved because of their importance for catalysis.[12] These residues are Glu57 and Cys84, which act as acids and bases in the cleavage mechanism. The crystal structure of LuxS from *Bacillus subtilis* has been characterized and demonstrated that the enzyme exists as a homodimer, which requires conformational changes of the N terminal residues 125-129 to access these active site residues.[12]

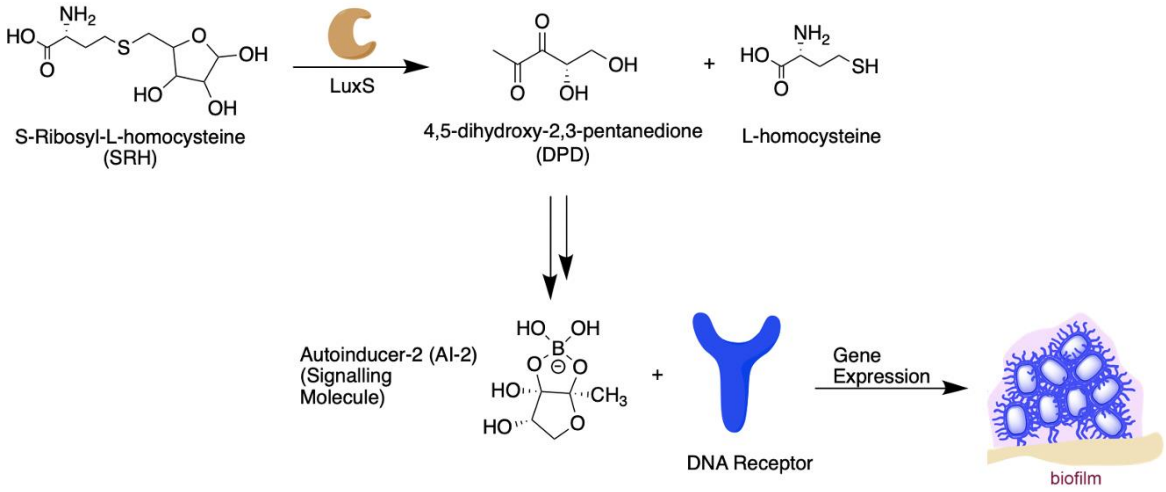

Figure 3. The pathway to autoinducer-2 as a signaling molecule in quorum sensing. SRH is the natural substrate that is cleaved by LuxS into DPD and homocysteine.

There has been some progress on synthesizing inhibitors of the LuxS enzyme in order to stop the production of AI-2 signaling molecules. Most of the previous inhibitors have been synthesized in order mimic the natural substrate.[13] Through mimicking the natural substrate, Alfaro *et al.* were able to inhibit the LuxS enzyme.[10] Inhibition of LuxS was quantified through enzyme based activity assays using Ellman's reagent, a disulfide compound that can interact with

the thiol of homocysteine. In one structure activity relationship study done by Shen *et al*., they found two inhibitors that contained the homocysteine moiety to be succcessful inhibitors of LuxS, with inhibitory constants of 0.72 and 0.37 μM, which are some of the most potent inhibitors of LuxS described previously.[14] When making derivatives with alterations to the homocysteine group, the inhibtory constants were well above 150 μM or the inhibitors demonstrated no inhibition at all. The results strongly indicated the importance of the homocysteine group on inhibitors for recognition by the LuxS enzyme. Interestingly, another study demonstrated that halogenated furanones isolated from marine red algae, which do not contain a homocysteine moiety, were found to inhibit LuxS (Figure 4A).[15] The compounds that showed the strongest inhibition were two compounds containing a vinyl monobromide, while the weaker compounds contained a vinyl gem-dibromide. The exact mechanism behind how these halogenated furanones inhibit the enzyme is unknown and needs to be studied further, yet a mechanism has been proposed involving covalent attachment. To test this, the inhibitor was incubated with LuxS and analyzed by mass spectrometry, in which they found the mass change matched the addition of the furanone with one less bromine atom. The enzyme was then digested with Glu-C endoprotease and trypsin to fragment the protein, which these fragments were analyzed by MALDI-Mass spectrometry. Unexpectedly, the results suggested that their inhibitor modified Cys126 and not Cys84, even though Cys84 normally exists as a thiolate with a pK_a of about 6 and is more solvent accessible than Cys126. Cys126 helps coordinate the metal for aldose-ketose isomerization in the regular mechanism, so alkylation of this residue likely reduces enzyme activity by blocking substrate binding or improper metal binding. In addition, a side experiment was performed by incubating LuxS with chloroacetone and the complex was again analyzed by mass spectrometry and found that acetone moieties had been added to all 4 cysteine residues.[15] The results from this study give evidence that the homocysteine group is not necessarily crucial for inhibition of LuxS and that both cysteine residues can be covalently modified either selectively or not, which provides motivation to better understand structure-activity relationships involved in LuxS binding.

Covalent inhibition has become an increasingly popular method of drug design. The advantage of covalent inhibition is that a bond is formed between the drug and the protein target. If this inhibitor acts irreversibly, this binding will overcome equilibrium kinetics and result in high efficiency. In addition, creating a covalent bond will decrease competition from the natural substrate.[16] Previous covalent inhibitors of quorum sensing have been accomplished in inhibiting the LasR pathway in *P. aeruginosa*.[13,17] The LasR pathway uses an AHL-like signaling molecule with LasR as the receptor for receiving this signal.[17] One study by Amara *et al.* synthesized isothiocyanate derivatives of the natural AHL-like substrate with varying chain lengths to act as covalent probes (Figure 4B).[17]

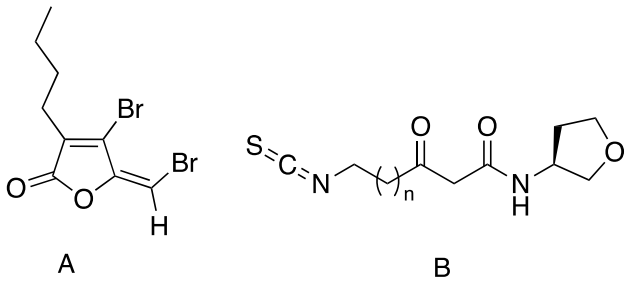

Figure 4. Previously synthesized inhibitors that have proposed mechanisms involving a covalent bond between the inhibitor and a cysteine residue within an enzyme. A refers to the covalent inhibitor that reacts with Cys84 within LuxS, and B refers to the inhibitor that reacts with Cys79 within LasR.[15,17]

They exploited a nucleophilic cysteine residue within LasR, Cys79, in hopes of achieving covalent inhibition. Inhibition of quorum sensing was evaluated by using a luminescent reporter strain of P. aeruginosa, which several isothiocyanates were found to strongly inhibit luminescence. To test a covalent mechanism of inhibition, a similar procedure using mass spectrometry was carried out as described above and determined that the probes were interacting with the desired Cys79 residue.[15,17] This study demonstrated that covalent inhibtion of quorum sensing is possible with a cysteine residue, and provides a basis to try similar experiments on other quorum sensing pathways, such as the AI-2 pathway.

With the rise of covalent inhibition as a potential drug strategy, many studies have investigated the relative reactivity and utility of various electrophiles. Electrophiles that are too reactive will be less specific and react with off-target residues, potentially causing deleterious effects. The reactivity of cysteine specifically as a nucleophile has been

probed in these studies due to high nucleophilicity of the sulfur.[18] In addition, it can exist within an active site in thiolate form, and cysteines are found in many enzyme active sites. One class of covalent drugs use α,β-unsaturated carbonyls as the electrophiles since they have relatively low reactivity, compared to something like an acyl chloride or anhydride, which are highly reactive with any nucleophile. Other potential low reactivity electrophiles are α-halocarbonyls, epoxides, and vinyl sulfonamides. By having low reactivity, the goal is to bind with the specific cysteine residue within the active sites of any target enzyme.[18]

The goal of this project is to synthesize new effective inhibitors of LuxS with the goal of inhibiting biofilm formation and elucidating more of the mechanism behind LuxS inhibition. The strategy that will be taken to accomplish this is covalent inhibition, by combining elements from all the previous studies described. Since LuxS has the highly conserved nucleophilic Cys84 in the active site, inhibitors that mimic the natural substrate will be synthesized with electrophilic groups attached in order to promote covalent inhibition (Figure 5).

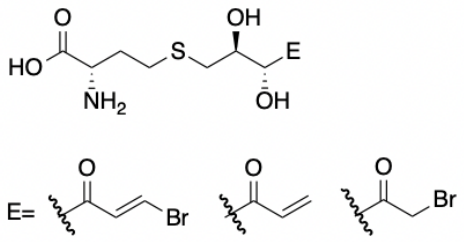

Figure 5. Potential Inhibitors to be synthesized with homocysteine as a scaffold and potential electrophilic groups to promote covalent inhibition.

By keeping homocysteine as a scaffold, this part of the molecule will lock it into the active site of LuxS, while the other part of the molecule will act as an electrophile to react with cysteine.

Specifically, the synthesis of an L-homocysteine derivative with an α,β-unsaturated carbonyl as the electrophile has been proposed for this project (Scheme 1). Once synthesized, LuxS will be introduced into *E. coli* via plasmid transformation and purified. Enzyme activity based assays will be run in order to test for inhibition of LuxS from synthesized inhibitors and biofilm inhibition will be tested through utilizing crystal violet assays.[19] As a method of antivirulence to combat antibiotic resistance, all these methods aim to inhibit quorum sensing in bacteria to ultimately stop formation of biofilms.

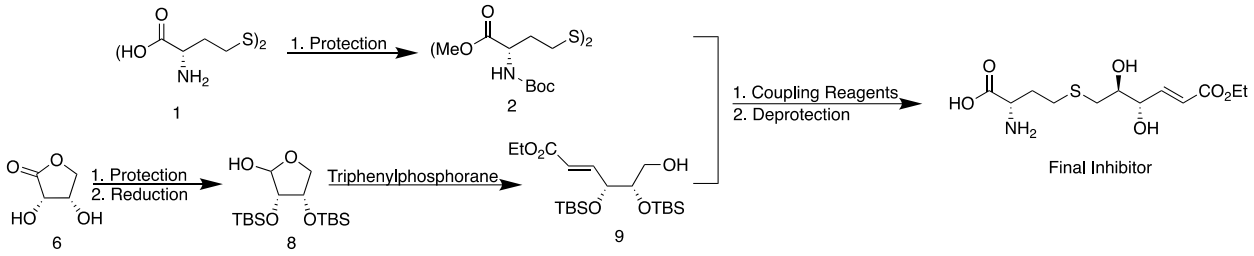

Scheme 1. Overall synthetic scheme to the proposed inhibitor of LuxS in this study.

2. Experimental Methodology

2.1 Chemical Synthesis General Methods.

Chemicals were purchased from either Alfa Aesar, Acros Organics, or Thermo Fisher Scientific. Anhydrous solvents were collected from a solvent purification system. Reactions were concentrated under reduced pressure using a rotary evaporator unless otherwise noted. Thin layer chromatography (TLC) was performed on SiliaPlate from Silicycle. Visualization was accomplished with short wave UV light (254 nm) or aqueous basic potassium permanganate solution followed by heating. Flash column chromatography was performed using silica gel (SiO_2, 40-63 µm, 230-400 mesh) purchased from Silicycle. Proton nuclear magnetic resonance spectra (^{1}H NMR) were recorded on a 400 MHz Varian NMR spectrometer with solvent resonance as the internal standard (^{1}H NMR: $CDCl_3$ at 7.27 ppm) unless otherwise stated. ^{1}H NMR data are reported as follows: chemical shift, multiplicity (s = singlet, d = doublet, t = triplet, q = quartet, dd = doublet of doublets, ddd = doublet of doublet of doublets, m = multiplet, br = broad) and integration.

2.2 Preparation of Protected L-homocysteine.

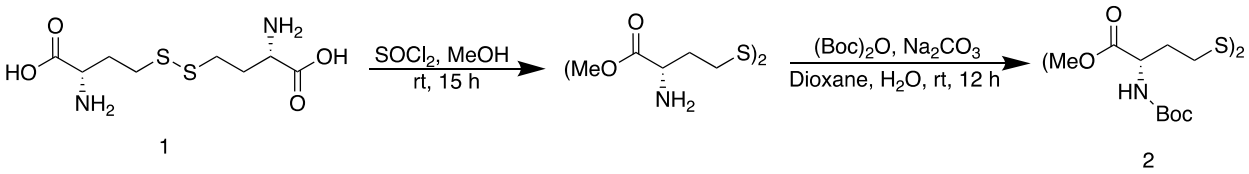

Scheme 2. Protection of carboxylic acid and amine in L-homocystine (**1**).

2.2.1 protection of L-homocystine.[10]

Thionyl chloride (1 mL) was added dropwise to anhydrous methanol (9.5 mL) under argon at 0°C. The reaction was left to stir for ten minutes. L-homocystine (**1**) (1 equiv, 0.93 mmol, 250.8 mg) was then added to the mixture and left to stir for 12 hours. The reaction mixture was then monitored by TLC and left to stir for an additional 3 hours. The reaction was then concentrated under air flow. Dioxane (2 mL) and water (1 mL) were then added to the reaction mixture. The pH of the reaction was changed by addition of 10% aqueous sodium carbonate solution until the pH reached about 7. While adding sodium carbonate, the reaction mixture changed from a yellow color to a reddish color and then settled at a black color. The reaction was cooled to 0 °C and di-tert-butyl dicarbonate (Boc_2O) (4.68 equiv, 4.35 mmol, 1.013 g) was added to the reaction. The pH was then tested and adjusted back to 7 using 10% sodium carbonate. The reaction was left to stir for 12 hours at room temperature. Then, the reaction mixture was extracted three times with dichloromethane and concentrated in vacuo. The reaction mixture was diluted with ethyl acetate, washed three times with saturated sodium bicarbonate, washed three times with saturated brine, and then dried with magnesium sulfate. The compound was purified via column chromatography (2:1 hexane:ethyl acetate). Purification afforded compound (**2**) as a white-yellowish solid (0.33 g, 0.76 mmol, 82%). TLC: R_f 0.9 (100% ethyl acetate, $KMnO_4$ stain); ^{1}H NMR ($CDCl_3$, 400 MHz): δ 1.4 (s, 18H), 2 (m, 2H), 2.3 (m, 2H), 2.7 (t, J = 7.6 Hz, 4H), 3.7 (s, 6H), 4.3 (m, 2H), 5.1 (d, J = 8.4 Hz, 2H). NMR peaks were consistent with reported values.[10]

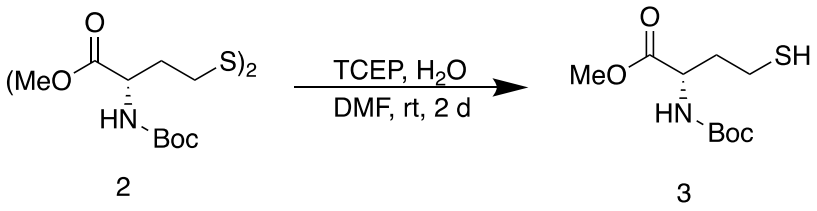

2 3

Scheme 3. Reduction of L-homocystine (**2**) to L-homocysteine (**3**).

2.2.2 reduction of protected L-homocystine.[20]

The protected L-homocystine (**2**) (1 equiv, 0.04027 mmol, 20 mg) was dissolved in anhydrous dimethylformamide (1.1845 mL, 0.01530 mol) in a small vial under argon. Deionized water (106 µL, 0.0059 mol) was added to the stirring reaction. Tris(2-carboxyethyl)phosphine (1.4 equiv, 0.05638 mmol, 14.1 mg) was then added to the reaction in one portion. The reaction was left to stir overnight at room temperature. After 24 hours, the reaction was monitored by TLC and left to stir overnight at room temperature for an additional 24 hours. The reaction was then diluted with ethyl acetate and saturated $NaHCO_3$. The organic layer was separated and washed with water 3 times and then brine. The combined organic layers were dried over $MgSO_4$ and concentrated in vacuo. This afforded product **3 (**0.0177 g**,** 0.0727 mmol**,** 87%) as a colorless oil. Following literature procedure, this product was of sufficient purity to be used in its next reaction.[20] TLC: R_f 0.30 (3:1 hexane:ethyl acetate, $KMnO_4$ stain) ^{1}H NMR ($CDCl_3$, 400 MHz): δ 5.10 (br, 1H), 4.2 (br, 1H), 3.75 (s, 3H), 2.70 (m, 2H), 2.10 (br, 1H), 1.90 (m, 1H), 1.51 (t, J = 9.6 Hz, 1H), 1.30 (m, 9H).

2.3 Preparation of Wittig Reagents.

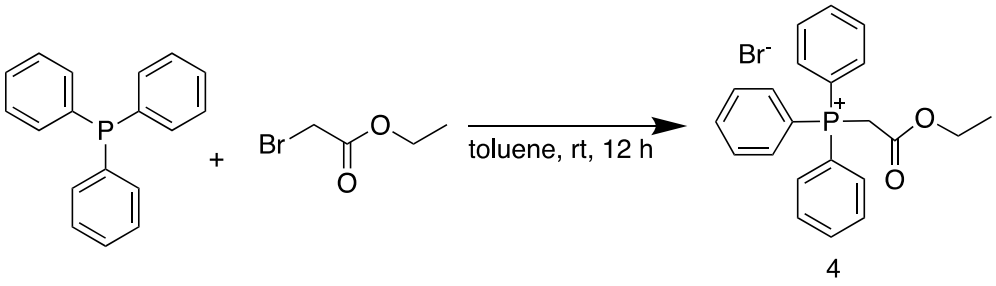

4

Scheme 4. Coupling of triphenyl phosphine and ethyl 2-bromoacetate.

2.3.1 preparation of (Ethoxycarbonylmethyl) triphenyl phosphonium bromide.[21]

Triphenylphosphine (1 equiv, 3.81 mmol, 1.0078 g) was dissolved in toluene (19.05 mL). Ethyl 2-bromoacetate (1 equiv, 3.81 mmol, 0.4 mL) was added to a separate vial with toluene (19.05 mL). The mixture of toluene and ethyl 2-bromoacetate was added dropwise to solution of triphenylphosphine under argon balloon over 10 minutes. The reaction was left to stir at room temperature for 12 hours. The reaction mixture was then filtered in a Buchner funnel and left to dry on the vacuum for 5 minutes. The reaction afforded the product (**4**) as a white powder (1.0161 g, 62%). ^{1}H NMR ($CDCl_3$, 400 MHz): δ 7-8 (m, 15H), 5.6 (d, J = 13.6 Hz, 2H), 4.1 (q, J = 7.2, 14.4 Hz, 2H), 1.1 (t, J = 7.6 Hz, 3H).

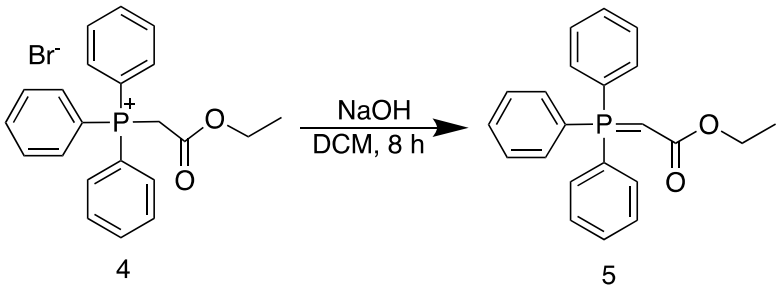

Scheme 5. Deprotonation of (ethoxycarbonylmethyl) triphenyl phosphonium bromide (**4**).

2.3.2 preparation of (Ethoxycarbonylmethyl) triphenylphosphorane.[22]

Triphenylphosphine salt (**4**) (1 equiv, 0.349 mmol, 0.1538 g) was dissolved in dichloromethane (1 mL). Sodium hydroxide (0.84 mL, 0.0318 mol) was added dropwise to the stirring solution. The reaction was left to stir vigorously for 15 minutes. Then, layers were separated, and the aqueous layer was extracted three times with dichloromethane. Organic layers were combined, dried over magnesium sulfate, and concentrated in vacuo. A crude NMR was taken and a critical peak at 2.9 ppm was missing. The reaction was redone using the same procedure, but this time the reaction was stirred for 8 hours rather than the reported 15 minutes.[22] The NMR taken for the new reaction showed DCM and water still present, so the product was dissolved in some dichloromethane, dried again over magnesium sulfate, filtered, and concentrated in vacuo. The resulting product was dried on the high vac for an additional 2 hours in order to afford the product (**5**) as a pale yellow solid (0.1028 g, 82%). This reaction was then later scaled up with **3** (0.6794 g, 1.584 mmol, 1 equiv) in dichloromethane (5.3 mL) and sodium hydroxide (4.2 mL, 0.1591 mol) using the same procedure to afford product (**5**) as a pale-yellow solid (0.5022 g, 91%) ^{1}H NMR ($CDCl_3$, 400 MHz): δ 7-8.00 (m, 15H), 3.9 (q, J = 7.6 Hz, 2H), 2.9 (br, 1H), 1.05 (t, 3H).

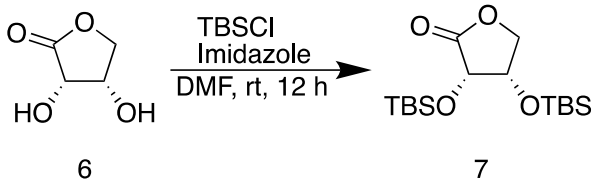

Scheme 6. Protection of D-erythronolactone (**6**) hydroxyl groups with TBS protecting groups.

2.3.3 protection of D-erythronolactone.[23]

A solution was created by dissolving lactone **6** (1 equiv, 7.62 mmol, 0.9138 g) in anhydrous dimethylformamide (37.6 mL, 0.4856 mol) and then cooled to 0°C. Imidazole (6 equiv, 45.73 mmol, 3.1138 g) was then added to the reaction mixture. Tert-butyldimethylsilyl chloride (6 equiv, 45.73 mmol, 6.8856 g) was added in one portion to the reaction mixture. The reaction mixture was left to stir under argon at room temperature for 12 hours. The reaction mixture was quenched with saturated aqueous ammonium chloride and then diluted with diethyl ether. Layers were separated and the aqueous layer was extracted two more times with diethyl ether. Organic layers were then combined and washed with water and saturated brine. The reaction mixture was dried over magnesium sulfate and then filtered and concentrated in vacuo. The product was purified via silica gel column chromatography using a 4:1 hexane:ethyl acetate system. Fractions were monitored by TLC using a 3:1 hexane:ethyl acetate mobile phase and fractions 1-12 were collected and concentrated in vacuo. The product analyzed by NMR had extra unidentifiable peaks near 1.6 ppm and integrations that did match with the literature, so TLC was run on the purified product to check for impurities. A 10:1 hexane:ethyl acetate mobile phase was used for all further TLCs. The product was stained with Anisaldehyde, Iodine, and 2,4-DNP stains but no spots were found. 55 mg of the purified product was taken and repurified via silica gel chromatography using a 10:1 hexane: ethyl acetate system. From TLC, it seemed as there were three separate spots, so three separate groups of fractions were collected, concentrated, and NMR samples were prepared using deuterated

chloroform. The first spot ended up correlating to the desired product. The rest of the purified product was repurified using the same conditions and beginning fractions from this column chromatography afforded the product (**7**) as a white solid (1.5923 g, 59%). TLC: R_f 0.4 (hexane:ethyl acetate 10:1, $KMnO_4$ stain) ^{1}H NMR ($CDCl_3$, 400 MHz): δ 4.4 (d, J = 2.4 Hz, 1H), 4.3 (dd, J = 2, 2 Hz, 1H), 4.25 (d, J = 9.6 Hz, 1H), 4.2 (d, J = 9.6 Hz, 1H), 0.9 (s, 9H), 0.8 (s, 9H), 0.3 (d, J = 2.8 Hz, 6H), 0.2 (d, J = 2.4 Hz, 6H).

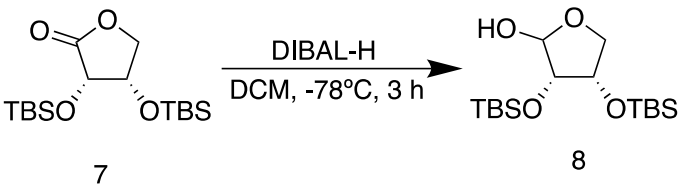

Scheme 7. Reduction of TBS protected D-erythronolactone (**7**) with DIBAL-H.

2.3.4 reduction of TBS protected D-erythronolactone.[23]

Lactone **7** (1 equiv, 1.44 mmol, 0.4995 g) was dissolved in anhydrous dichloromethane (7.21 mL, 0.1125 mol) and cooled to -78ºC. DIBAL-H (3 equiv, 4.33 mmol, 4.3 mL, 1.0 M solution in heptane) was added dropwise to the cooled stirring solution under an argon balloon. The reaction was left to stir at this temperature for three hours. A saturated solution of Rochelle's salt was prepared by dissolving potassium sodium tartrate in water until saturated. After 3 hours, the reaction was quenched with saturated aqueous Rochelle's salt (10 mL) and diluted with dichloromethane (10 mL). The reaction mixture was left to stir at room temperature overnight. Layers were then separated, and the aqueous layer was extracted with dichloromethane three times. Organic layers were combined and washed with water and brine successively, dried over magnesium sulfate, filtered, and concentrated in vacuo. Silica gel chromatography was run using a 10:1 hexane:ethyl acetate system to purify the product. Fractions were collected and concentrated in vacuo to afford the product **8** as a colorless residue (0.2183 g, 44%). TLC: R_f 0.30, 0.35 (10:1 hexane:ethyl acetate, $KMnO_4$ stain); ^{1}H NMR ($CDCl_3$, 400 MHz): Small peak around δ 9.3 ppm that could correspond to aldehyde form, δ 5.02 (dd, J = 4, 11.2 Hz, 1H), 4.20 (d, J = 43.2 Hz, 1H), 4.15 (m, 1H), 3.94 (dd, J = 4, 8.4 Hz, 1H), 3.89 (m, 2H), 0.8-0.9 (m, 18H), 0.05-0.20 (m, 12H).

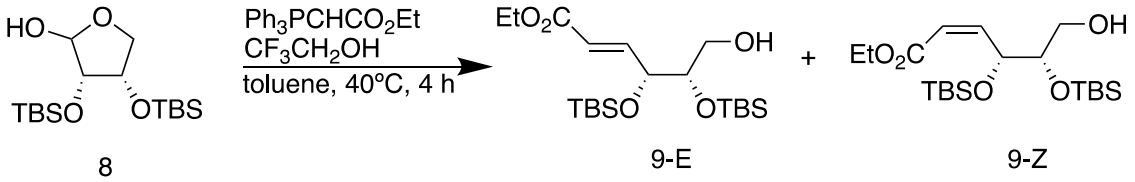

Scheme 8. Wittig reaction of TBS-protected reduced lactone (**8**) and (ethoxycarbonylmethyl) triphenylphosphorane.

2.3.5 wittig reaction of tbs-protected reduced lactone and (ethoxycarbonylmethyl) triphenylphosphorane.[23]

The reduced lactone (**8**) (1 equiv, 0.1471 mmol, 0.0513 g) was dissolved in anhydrous toluene (1.5 mL, 0.0141 mol). This solution was transferred to a small vial and stirred under an argon balloon. 2,2,2-trifluoroethanol (2 equiv, 0.2943 mmol, 0.021mL) was added dropwise to the reaction solution followed by adding the ethyl acetate triphenyl phosphorane **(5)** (1 equiv, 0.1471 mmol, 0.0509 g) in one portion. The reaction flask was warmed to 40ºC in an oil bath. The reaction was monitored by TLC (10:1 hexane:ethyl acetate, $KMnO_4$) and stopped after 4 hours of stirring. The reaction mixture was quenched by adding a few drops of saturated ammonium chloride and was then diluted with ethyl acetate. This reaction mixture was then transferred to a bigger vial and layers were separated. The aqueous layer was extracted three times with ethyl acetate and organic layers were combined, dried over magnesium sulfate, filtered, and concentrated in vacuo. The product was purified using a 20:1 hexane:ethyl acetate solvent system to completely separate the E and Z isomers as colorless residues (0.2151 g, 82%, 4:1 E:Z). For **9-E**: TLC: R_f 0.25 (hexane:ethyl

acetate 10:1, UV, $KMnO_4$) ^1H NMR ($CDCl_3$, 400 MHz): δ 6.99 (dd, 5.6, 15.6 Hz, 1H), 5.99 (dd, J = 1.6, 15.6 Hz, 1H), 4.25 (dd, J = 1.6, 5.2 Hz, 1H), 4.17 (q, J = 6.3, 7.2 Hz, 2H), 4.07 (q, J = 6.8 Hz, 1H), 3.78 (m, 1H), 3,5-3.6 (m, 2H), 1.99 (dd, J = 4, 9.2 Hz, 1H), 1.3 (m, 3H), 1.0 (m, 18H), 0.08-0 (m, 12H). For **9-Z**: TLC: R_f 0.40 (hexane:ethyl acetate 10:1, UV, $KMnO_4$) ^1H NMR ($CDCl_3$, 400 MHz): δ 6.20 (dd, J = 8.8, 12 Hz, 1H), 5.91 (dd, J = 1.2, 11.6 Hz, 1H), 5.50 (m, 1H), 4.15 (q, J = 6.8, 14.4 Hz, 2H), 3.80-3.90 (m, 1H), 3.5-3.6 (m, 1H), 3.35-3.45 (m, 1H), 3.20 (q, J = 5.2, 9.2 Hz, 2H), 1.30 (dd, 3H), 0.9 (m, 18H), 0.05-0.1 (d, J = 1.36 Hz, 6H), 0.01-0.05 (d, J = 2.8 Hz, 6H).

2.4 Coupling Steps

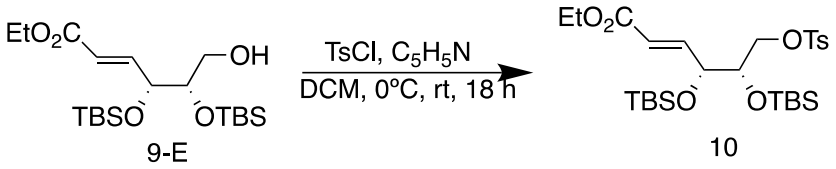

Scheme 9. Tosylation of Wittig Product **9-E**.

2.4.1 tosylation of wittig product.[24]

The Wittig product (**9-E**) (1 equiv, 0.2388 mmol, 0.1027 g) was dissolved in anhydrous dichloromethane (0.24 mL, 0.0037 mol). The reaction mixture was cooled to 0°C in an ice bath under an argon balloon. P-toluenesulfonyl chloride (1.1 equiv, 0.2627 mmol, 0.00503 g) was added to the reaction mixture. Pyridine (1.1 equiv, 0.2627 mmol, 21 µL) was added to the reaction mixture. The reaction was then warmed to room temperature and then left to stir for three hours. After 3 hours, the reaction was monitored by TLC and then left to stir overnight. The reaction was then quenched with saturated aqueous ammonium chloride and diluted with water. The quenched mixture was than extracted 3 times with dichloromethane and organic layers were combined, dried over $MgSO_4$ and concentrated in vacuo. A crude TLC (10:1 hexane:ethyl acetate) was performed and three spots appeared close to each other, so the product was purified with a more nonpolar solvent (20:1 hexane:ethyl acetate). Fractions were completely separated and concentrated under vacuo, which afforded the product (**10**) as a colorless oil (0.0457 g, 34%). TLC: R_f 0.30 (10:1 hexane:ethyl acetate, UV). ^1H NMR ($CDCl_3$, 400 MHz): δ 7.80 (dd, J = 2, 6.8 Hz, 2H), 7.3 (dd, J = 0.8, 8.4 Hz, 2H) 6.99 (dd, J = 5.6, 16 Hz, 1H), 5.99 (dd, J = 1.6, 15.6 Hz, 1H), 4.25 (m, 1H), 4.17 (q, J = 7.2, 14.4 Hz, 2H), 4.07 (m, 1H), 3.78 (m, 1H), 3,5-3.6 (m, 2H), 2.5 (s, 3H), 1.99 (m, 1H), 1.3 (dd, J = 7.2, 11.6 Hz, 3H), 1.0 (m, 18H), 0.08-0 (m, 12H).

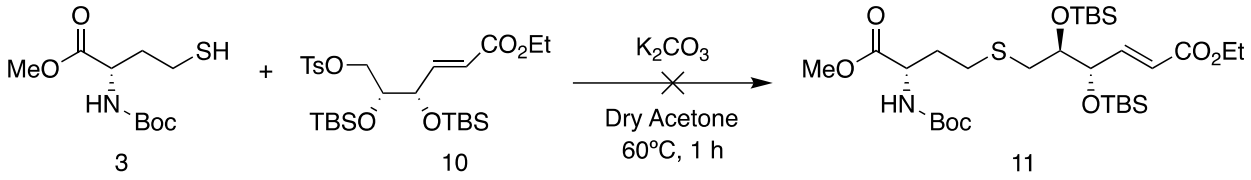

Scheme 10. Unsuccessful attempt at coupling protected L-homocystine (**3**) to tosylation product (**10)**.

2.4.2 coupling of protected l-homocysteine to tosylation product.[20]

Thiol **3** (1 equiv, 0.0244 mmol, 6.1 mg) was dissolved in acetone (3 mL, 0.0409 mol) that was dried over 3 Å molecular sieves. The mixture was transferred to a flask and tosylated product **10** (1.25 equiv, 0.0305 mmol, 17.5 mg) was added to the mixture in one portion. Potassium carbonate (7.25 equiv, 0.1772 mmol, 0.0245 g) was added to reaction and stirred. The heterogenous mixture was placed into a 60 ºC oil bath and refluxed for 1 hour under argon. After one hour, volatiles were evaporated in vacuo. The reaction was diluted with ethyl acetate and then washed with saturated $NaHCO_3$. The organic layer was dried over $MgSO_4$ and concentrated again. An NMR sample was prepared with deuterated chloroform. TLC (4:1 hexane:ethyl acetate $KMnO_4$ stain) showed four spots (R_f: 0.10, 0.15, 0.20, 0.40) and the NMR spectrum showed all starting material peaks that were not shifted, so no reaction took place.

2.5 Biochemical Synthesis General Methods.

Biological reagents were purchased from either Alfa Aesar, Acros Organics, or Thermo Fisher Scientific. All sterile equipment was sterilized using an autoclave or passing liquid through a 0.22 μm syringe filter. Biological kits were purchased from New England Biolabs (NEB), and protocols were adapted from given procedures. Samples were centrifuged at 16,000x g (13,000 RPM) unless stated otherwise. For shaking incubations, samples were incubated in a New Brunswick Excella E25 Incubator Shaker. For non-shaking incubation, a general-purpose incubator for Barnstead Lab-Line was used. For reactions requiring a thermocycler, a BIO-RAD T100 Thermal Cycler was used. DNA was quantified using a NanoDrop microvolume spectrophotometer. LB medium (yeast extract, tryptone, NaCl, and water) was used for liquid cultures and agar plates. For protein expression, minimal media was used, consisting of M9 Salts (3 g/L KH_2PO_4, 12.8 g/L $Na_2HPO_4{\cdot}7H_2O$, .5 g/L NaCl, 1 g/L NH_4Cl), a metal salt mixture (0.5 mM $MgSO_4$, 0.5 μM H_3BO_3, 0.1 μM MnCl2, 0.5 μM $CaCl_2$, 10 μM $CuSO_4$, 1 nM ammonium molybdate), 0.25% D-glucose, 2 μg/mL thiamin, 1 μg/mL D-biotin, and 0.1% $(NH_4)_2SO_4$.[25] Medias were supplemented with 50 μg/mL of ampicillin. Gel electrophoresis was ran at 90V using a TAE buffer (.8 mM tris free base, .04 mM disodium EDTA, and 0.4 mM glacial acetic acid) and a 1% gel consisting of agarose in TAE buffer and 2.5 μL of 10 mg/mL ethidium bromide. NEB Quick-Load 1 kb Plus DNA ladder was used as ladder in all gel electrophoresis experiments.

2.6 Creation of pET22b-luxs-HT.

Plasmid pET-22b(+) was transformed and amplified into competent DH5α *E. Coli* cells using SOC outgrowth media plated onto selective ampicillin plates. The amplified plasmid was purified from a 2 mL LB liquid culture according to the NEB Miniprep Kit. The plasmid was cut by incubating it with *NdeI* and *XhoI* restriction enzymes overnight in CutSmart buffer to produce linearized DNA, which was verified by gel electrophoresis. A ligation reaction was performed on the linearized DNA using HiFi DNA master mix and a gBlock containing the sequence for the *luxs* gene to insert the gene near a C-terminal Histidine tag for purification (sequence: 5'-TGGTGGTGGTGGTGCCCGCCAAATACTTTTAGCAATTCTTCTTTATCCTGTGAAAGCCAGAAACGCATT AAACGTTTAGCGCCTTCCAGATCATGAAGCTTCGCTTGGCCGCACTGCTTTTCATTCGCAGCAGGTATT TCTGTAATCTCTACCGCTTCCTTCATTGTGTCTTCAAGCAGATCAACGATTTCCGCTGATGTCGGCTCTC CGCTCACAACTAGATAATAGCCTGTCTGGCAGCCCATTGGAGAAATATCAATGATATCAAAATGATCG TATTTCTCAGCGTGAGAACGAATCGTAAACGCGAGCAAATGCTCGAGTGTGTGAATGGTGTCAGGCTT CATCGCCTGTTTATTTGGCTGGCAAAAACGAATGTCAAATTTATTTACAACGCCGTCTGTTCCCACTTT ATGCACGCCGCAATGTCTTACATATGGAGCAACAACCGCATTATGATCAAGCTCAAAACTTTCTACTG AAGGCATTGTATATCTCCTTCTTAAA-3'). The resultant plasmid was transformed into competent DH5α *E. Coli* cells, plated, and purified using the same conditions as described above.

2.7 Diagnostic analysis of pET22b-luxs-HT.

To confirm the identity of the plasmid, a restriction enzyme digest was ran on the purified pET22b-luxs-HT from the ligation reaction using the same enzymes, *NdeI* and *XhoI*, and gel electrophoresis was ran to visualize results. For further verification, colony PCR was conducted on the transformed pET22b-luxs-HT DH5α *E. Coli* cells by diluting a colony in water and using the Q5 high-fidelity master mix. The primers used for PCR were as follows: T7 promoter, 5'-TAATACGACTCACTATAGGG-3' and T7 terminator, 5'-GCTAGTTATTGCTCAGCGG-3'. Whole plasmid samples and PCR fragments were sent to Genomic Sciences Laboratory at NC State University to be sequenced, which verified the identity of the plasmid construction.

3. Results and Discussion

Looking at the first half of the proposed scheme, the protected L-homocystine (**2)** was successfully synthesized with an 82% yield (0.33g). NMR data confirmed the identity of this compound, according to literature values.[10] The reduction of the disulfide to afford the thiol **3** took some troubleshooting. Originally, likely due to running the reaction on a small scale, it was hard to tell from the NMR spectrum if any reaction had taken place due to the similarity of the starting material and product. Since the coupling step uses up material that was not synthesized in excess, it was decided to rerun the reaction. The reaction procedure was reran now waiting an additional 24 hours than what the

procedure called for.[20] The longer reaction time resulted in the thiol in 82% yield (0.0177 g) confirmed by the thiol peak near 1.5 ppm in the proton NMR spectrum. Since all that is changing within this reaction is the breakage of the disulfide, it is difficult to say with certainty whether or not the product was pure from just looking at the NMR spectrum. However, it was decided to use this product in its next step to see if the coupling reaction could take place.

For the other half of the proposed synthesis, the Wittig reagents needed to be prepared. NMR confirmed that the triphenylphosphine salt (**4**) was successfully synthesized, and after a second longer attempt at deprotonation, the salt was successfully transformed to the ylide (**5**). After troubleshooting the purification, the tert-butyldimethylsilyl protected lactone (**7**) was also successfully synthesized. The NMR for this product had high integration near 0 ppm that is likely silica grease and the chloroform and TMS standard peaks had unusual splitting due to the concentration of sample, but other peaks matched the literature, so the product (**7**) was used for the next step. The yield for this product (**7**) was a moderate 59% yield, which product was likely lost due to impurities of similar R_f and the need for multiple purifications. The protected lactone (**7**) was successfully reduced (**8**) with a moderate 44% yield. The results from TLC showed two spots with R_f values of 0.30 and 0.35, which are likely the α/β forms as the NMR spectrum did not show any large impurities or unknown peaks. These two different isomers form because the reduction makes that carbon an anomeric carbon. The α/β ratio seen in the NMR spectrum changed from the first purification to the second purification. This could be explained by a loss of 1 form in product during the second purification or interconversion between the two catalyzed by acidic silica, which would account for the change in ratio and a lower yield.

This product was used for the Wittig reaction along with the ylide (**5**). This reaction proceeded smoothly to afford the product (**9**) with a high 82% yield. The results from TLC and NMR also confirmed that two different isomers of the E and Z alkene were produced, and through column chromatography, the two different isomers were able to be completely separated from one another for an E:Z ratio of 4:1. The identity of each isomer was confirmed by NMR, as the E isomer had alkene peaks more downfield than the Z isomer and the J coupling constants were larger for the E isomer, both of which are characteristic of trans alkenes. All Wittig precursor reactions and the Wittig reaction itself were redone for higher yields and all demonstrated reproducibility. It was then decided to use the E isomer for subsequent reactions simply because there was more product for that isomer but going back and creating the same inhibitor with the Z isomer is of interest to evaluate any potential effects of different orientation. Tosylation of the E isomer did occur and resulted in a low 34 % yield of the product (**10**). The three spots that showed up from crude TLC were able to be completely separated from each through column chromatography and were analyzed by NMR. The NMR spectra showed that the first spot off the column was tosyl chloride itself, the second spot was the desired product, and the last spot was unreacted starting material. Due to this analysis, it was concluded that the low yield was likely due to using old pyridine that was not completely dry, so water likely reacted with tosyl chloride as a competing reaction. When redoing this reaction, it will be ensured that completely dry pyridine is used for the reaction, which should help increase product yield. However, there was enough product to run the following reactions in order to see if synthesis of the proposed inhibitor is possible.

The coupling reaction between the protected L-homocysteine (**3**) and tosylated product (**10**) did not occur, as all starting material peaks were still present unshifted in the NMR spectrum after extraction. However, the thiol peaks were now absent or in very low concentration. The reaction likely did not occur because such low amounts were used with what had been synthesized previously. Going back and upscaling the reaction should be able to provide a better idea of whether or not this coupling could occur. In addition, the reaction could be heated and left running for a longer time to ensure full coupling of the reactants. Multiple different synthetic routes have been explored, so the possibility of using different and stronger bases to deprotonate the thiol could also be tested.[26]

The compounds synthesized herein provide crucial foundations for the final reactions that will be performed. These compounds will lead to the eventual completion of a potential inhibitor that can be tested for the possibility of covalent inhibition of LuxS. In addition, since this pathway is thus far successful except for the last reaction, these syntheses can be repeated and modified to synthesize new compounds with different electrophilic groups so that the possibility of covalent inhibition of LuxS by differing inhibitors can be evaluated. For example, from the protected lactone (**7**) a Wittig reaction can take place directly from the product to get a new derivative or reacted with carbon tetrabromide to get a vinyl dibromide derivative. In addition, sulfur could be replaced with oxygen. Right now, the end goal will be synthesis of an inhibitor with an α,β-unsaturated carbonyl as the electrophile to react with cysteine within the enzyme. However, synthesizing new derivatives with different electrophilic groups will also allow us to determine if one electrophile works best for possible covalent inhibition of the LuxS enzyme and each derivative can be used to inform future synthesis.

To test these inhibitors, the enzyme LuxS is needed. The plan to achieve this is by using the pET-22b(+) plasmid, which has an inducible lac operon and histidine tag for purification. This plasmid was successfully transformed into DH5α cells and amplified by the cells to a new concentration of 225.1 ng/μL. This process showed reproducibility, as two more amplified stocks of 149.4 ng/μL and 97.4 ng/μL were extracted and quantified. To create overlaps with the

luxs gene fragment, the plasmid was digested with *XhoI* and *NdeI* restriction enzymes. This reaction was evaluated by gel electrophoresis (Figure 6). The gel demonstrated that the stock solution showed characteristic bands of coiled and uncoiled DNA expected from a plasmid (Figure 6, Lane 2).

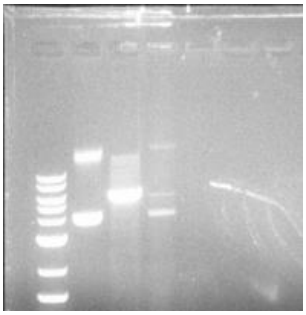

Figure 6. Gel electrophoresis of restriction enzyme reaction. Lane 1 contains the ladder, lane 2 the stock plasmid band near 5 kb, lane 3 the digested plasmid with a band near 4 kb, and lane 4 the original miniprep plasmid with middle band near 4 kb and bottom band near 5 kb.

The digested plasmid was linearized by the presence of only one band, however, the small DNA fragment cut out was not seen on the gel (Figure 6, Lane 3). This means that only one enzyme cut the DNA, or the smaller fragment was too small and could not be visualized on the gel. Smearing on the gel is from loading too high a DNA concentration onto the gel. The cleaned-up DNA from the restriction reaction afforded 64.3 ng/μL of DNA. It was decided to proceed with the ligation step. From the transformation of the ligated plasmids, the negative control had one small colony while the positive control matched the growth of the ligation plates, which means that colonies with DNA from the ligation reaction were able to grow.

Initially, the sequencing results came back with very high background and the sequence that was discernible was very short and not useful. It was decided to run multiple different diagnostic tests on the plasmid to see whether or not this issue was just a sequencing problem or with the plasmid itself. Since the *luxs* gene has the same restriction enzyme sites as the whole plasmid and the original sites would be gone with the addition of the gene, the restriction enzyme digest was repeated with the same enzymes, to see if the plasmid would be cut. In addition, 2 control reactions were added that only contained one of the enzymes to see if each enzyme was working properly. The original pET-22b(+) digestion with *XhoI* and *NdeI* was reran as well so that there would be a backup linearized plasmid if the problem was with the actual ligated plasmid and not a sequencing issue. As visualized by the gel, the ligated plasmid was successfully cut and both individual enzymes were cut, suggesting that the enzymes were working well and that the *luxs* gene was inserted (Figure 7, Lanes 3-5). In addition, the original pET-22b(+) plasmid was able to be cut again (Figure 7, Lane 7), so another ligation and transformation was performed on that.

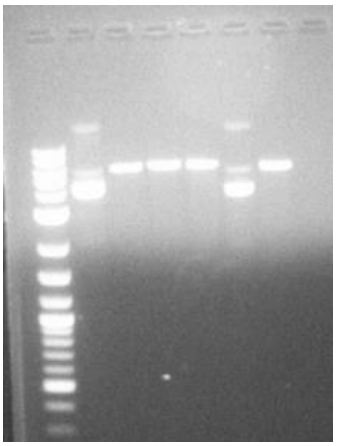

Figure 7. Gel electrophoresis of diagnostic restriction enzyme digests. Lane 1-Ladder, Lane 2- pET22b-luxs-HT middle band near 5 kb and bottom band 6 kb, Lane 3- pET22b-luxs-HT both enzymes- near 5 kb, Lane 4- pET22b-luxs-HT *NdeI* only near 5 kb, Lane 5- pET22b-luxs-HT *XhoI* only near 5 kb, Lane 6- pET-22b(+) HT middle band near 5 kb and bottom band 6 kb, Lane 7- pET-22b(+) digested near 5 kb.

The small cut out fragment did not appear for either plasmid, which confirms that it was just too small to see. The ligated plasmid also appeared to be slightly higher on the gel, which was expected as the *luxs* gene add more base pairs to the original plasmid.

For even further verification of the ligation being successful, and to possibly have easier templates to sequence, colony PCR was ran. For a control, PCR was ran on the original pET-22b(+) plasmid. Four different colonies that held the newly ligated plasmid were selected to run the PCR in case of a potential colony-to-colony issue. These four colonies were streaked and plated on selective plates separately to have isolated clones. As seen by visualization of the PCR products, the four colonies from the ligated plasmid showed a single band near 600 bp, which was the expected value for the PCR fragment containing the *luxs* gene (Figure 8, Lanes 3-6).

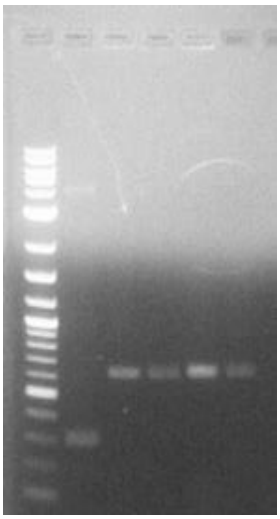

Figure 8. Gel electrophoresis of Colony PCR. Lane 1- Ladder, Lane 2- pET-22b(+) near 300 bp, Lanes 3-6, pET22b(+)-luxs-HT from colonies 1-4 respectively near 600 bp.

In addition, the original pET-22b(+) plasmid had a band near 300 bp, which was the expected size of this PCR fragment (Figure 8, Lane 2). These fragments demonstrated a clear difference between the two, which only further

confirmed that the desired gene had been successfully ligated. These PCR fragments were sent to be sequenced, as whole plasmids can often be difficult to sequence. However, multiple whole plasmids were also sent to be sequenced. From sequencing, the PCR fragments demonstrated the correct sequence, and one out of the three plasmids sent were able to get a decent sequence read with low background. All of the sequences confirmed that the desired gene had been successfully integrated with the histidine tag and start codon still intact. These results confirmed that likely the original issue was simply from sequencing problems in that the DNA itself was impure, or because the samples got damaged on the way there.

4. Conclusion

The synthesis described herein has created a foundation for the development of new potential LuxS inhibitors. Such molecules will provide the opportunity to test for covalent inhibition of LuxS with irreversible binding. Only a few inhibitors have been previously proposed to have a covalent mechanism with LuxS, so this study has provided further exploration into the topic. Optimization of covalent inhibitors of LuxS could provide an avenue toward anti-biofilm drugs that circumvent the growing problem of antibiotic resistance. In addition, changes can be made from the overall scheme to create derivatives with varying electrophilic groups in order to create a library of inhibitors to test. A plasmid for LuxS expression has successfully been made, so further steps to be done involve expression and purification of the protein to be used for enzyme activity assays. With a library of inhibitors to test, structure activity relationships can be done in order to find the optimal conditions for LuxS binding and further explore the binding interactions within the active site.

5. Acknowledgements

The author would like to express their gratitude to Dr. Caitlin McMahon and the McMahon lab for all their help and support during this project; the Department of Chemistry & Biochemistry, the Chemistry Scholars Program and Undergraduate Research Program for funding; Dr. Ryan Steed and Dr. Melinda Grosser for their help in planning and troubleshooting biology related issues; and Dr. Amanda Wolfe, Dr. Ted Meigs, and Dr. Melanie Heying for borrowing supplies and equipment.

6. References

1. Antibiotic/Antimicrobial Resistance | CDC. https://www.cdc.gov/drugresistance/index.html
2. Dickey, S. W.; Cheung, G. Y. C.; Otto, M. *Nat. Rev. Drug Discov.* **2017**, *16* (7), 457–471.
3. Totsika, M. *Drug Deliv. Lett.* **2016**, *6* (1), 30–37.
4. Roy, R.; Tiwari, M.; Donelli, G.; Tiwari, V. *Virulence* **2018**, *9* (1), 522–554.
5. Høiby, N.; Bjarnsholt, T.; Givskov, M.; Molin, S.; Ciofu, O. *Int. J. Antimicrob. Agents* **2010**, *35* (4), 322–332.
6. Bjarnsholt, T. *APMIS* **2013**, *121*, 1-58.
7. Khatoon, Z.; McTiernan, C. D.; Suuronen, E. J.; T. F.; Alarcon, E. I. *Heliyon* **2018**, *4(12)*, 1-36.
8. Sommer, R.; Joachim, I.; Wagner, S.; Titz, A. *Chim. Int. J. Chem.* **2013**, *67* (4), 286–290.
9. De Keersmaecker, S. C. J.; Sonck, K.; Vanderleyden, J. *Trends Microbiol.* **2006**, *14* (3), 114–119.
10. Alfaro, J. F.; Zhang, T.; Wynn, D. P.; Karschner, E. L.; Zhou, Z. S. *Org. Lett.* **2004**, *6* (18), 3043–3046.
11. Miller, S. T.; Xavier, K. B.; Campagna, S. R.; Taga, M. E.; Semmelhack, M. F.; Bassler, B. L.; Hughson, F. M. *Molecular Cell* **2004**, *15* (5), 677–687.
12. Ruzheinikov, S. N.; Das, S. K.; Sedelnikova, S. E.; Foster, A. H. S. J.; Horsburgh, M. J.; Cox, A. G.; McCleod, C. W.; Mekhalfia, A.; Blackburn, G. M.; Rice, D. W.; Baker, P. J. *J. Mol. Biol.* **2001**, *313* (1), 111-122.
13. Mina, G.; Chbib, C. *Bioorg. Med. Chem.* **2019**, *27* (1), 36–42.
14. Shen, G.; Rajan, R.; Zhu, J.; Bell, C. E.; Pei, D. *J. Med. Chem.* **2006**, *49* (10), 3003–3011.
15. Zang, T.; Lee, B. W. K.; Cannon, L. M.; Ritter, K. A.; Dai, S.; Ren, D.; Wood, T. K.; Zhou, Z. S. *Bioorg. Med. Chem. Lett.* **2009**, *19* (21), 6200–6204.

16. Bauer, R. A. *Drug Discov. Today* **2015**, *20* (9), 1061–1073.
17. Amara, N.; Mashiach, R.; Amar, D.; Krief, P.; Spieser, S. A. H.; Bottomley, M. J.; Aharoni, A.; Meijler, M. M. *J. Am. Chem. Soc.* **2009**, *131* (30), 10610–10619.
18. Long, M. J. C.; Aye, Y. *Cell Chemical Biology* **2017**, *24* (7), 787–800.
19. Cady, N. C.; McKean, K. A.; Behnke, J.; Kubec, R.; Mosier, A. P.; Kasper, S. H.; Burz, D. S.; Musah, R. A. *PLoS One* **2012**, *7* (6).
20. Chbib, C. *Bioorg. Med. Chem. Lett* **2017**, *27* (8), 1681-1685
21. Liu, Q.; Wang, J.; Li, D.; Yang, C.; Xia, W. *J Org Chem* **2017**, *82* (3), 1389–1402.
22. Dong, M.; Horitani, M.; Dzikovski, B.; Pandelia M. E.; Krebs, C.; Freed, J. H.; Hoffman, B. M.; Lin, H. *J Am Chem Soc.* **2016**, *138* (31), 9755-9758.
23. Sahu, P. K.; Kim, G.; Yu, J.; Ahn, J. Y.; Song, J.; Choi, Y.; Jin, X.; Kim, J.; Lee, S. K.; Park, S.; Jeong, L. S. *Org. Lett.* **2014,** *16* (21), 5796–5799.
24. Moussa, I. A.; Banister, S. D.; Beinat, C.; Giboureau, N.; Reynolds, A. J.; Kassiou, M. *J. Med. Chem.* **2010,** *53* (16), 6228–6239.
25. Zhu, J.; Dizin, E.; Hu, X.; Wavreille, A.-S.; Park, J.; Pei, D. *Biochemistry* **2003**, *42*(16), 4717–4726.
26. Bolitho, M. E.; Corcoran, B. J.; Showell-Rouse, E. I.; Wang K. Q. *Carbohydrate Research* **2014**, *394*, 32-38.